A. Findlay (1951). *The Phase Rule and Its Applications*, 9th Ed Dover N.Y.
P. Gordon (1968). *Principles of Phase Diagrams in Materials Systems*, McGraw-Hill, New York.
Phase Diagrams for Ceramists 1964 ed., 1969 Suppl., 1975 Suppl., 1981 Suppl., American Ceramic Society, Columbus, Ohio. The standard work of reference for phase diagrams of non-metallic inorganic materials.
A. Reisman (1970). *Phase Equilibria*, Academic Press, New York.
J. E. Ricci (1966). *The Phase Rule and Heterogeneous Equilibrium*, Dover, New York.
F. Tamas and I. Pal (1970). *Phase Equilibria Spatial Diagrams*, Butterworths 1970.

Chapter 12

Phase Transitions

Phase transitions are important in most areas of solid state science. They are interesting academically, e.g. a considerable slice of current research in solid state physics concerns soft mode theory, which is one aspect of phase transitions, and they are important technologically, e.g. in the synthesis of diamond from graphite, the processes for strengthening of steel and the properties of ferroelectricity and ferromagnetism. This chapter discusses structural, thermodynamic and kinetic aspects of phase transitions and their classification. A few of the more important phase transitions are described; others are mentioned elsewhere in this book.

12.1 What is a phase transition?

If a crystalline material is capable of existing in two or more polymorphic forms (e.g. diamond and graphite), the process of transformation from one polymorph to another is a phase transition. The terms *transition* and *transformation* are both used to describe this and are interchangeable. In the narrowest

sense, phase transitions are restricted to changes in structure only, without any changes in composition, i.e. to changes in elements or single phase materials. A much wider definition that is sometimes used includes the possibility of compositional changes, in which case more than one phase may be present before and/or after the transition. However, one then has to try and draw a dividing line between polymorphic transitions, on the one hand, and chemical reactions, on the other. The easiest solution is probably to try and avoid giving a precise definition of phase transitions!

Phase transitions are affected by both thermodynamic and kinetic factors. Thermodynamics gives the behaviour that should be observed under equilibrium conditions and, for a particular material or system, this information is represented by the phase diagram. Phase transitions occur as a response to a change in conditions, usually temperature or pressure but sometimes composition. The rates at which transitions occur i.e. kinetics, are governed by various factors. Transitions that proceed by a nucleation and growth mechanism are often slow because the rate controlling step, which is usually nucleation, is difficult. In martensitic and displacive phase transitions, nucleation is easy, occurs spontaneously and the rates of transition are usually fast.

12.2 Buerger's classification: reconstructive and displacive transitions

We can begin with the classification scheme of Buerger (1961) which initially divides phase transitions into two groups: reconstructive and displacive transitions. *Reconstructive* transitions involve a major reorganization of the crystal structure, in which many bonds have to be broken and new bonds formed. The transition, graphite⇌diamond, is reconstructive and involves a complete change in crystal structure, from the hexagonal sheets of three-coordinated carbon atoms in graphite to the infinite framework of four-coordinated carbon atoms in diamond, and vice versa. The quartz⇌cristobalite transition in SiO_2 is also reconstructive because although there is no difference in coordination between the two polymorphs—both structures are built of SiO_4 tetrahedra linked at their corners to form a three-dimensional framework—the polymorphs have different types of framework structure and many Si—O bonds must break and reform in order that the transition may take place. Because many bonds must break, reconstructive transitions usually have high activation energies and, therefore, take place only slowly.

Often, reconstructive transitions may be prevented from occurring, in which case the untransformed phase is kinetically stable although thermodynamically it is metastable. A classic example is the occurrence of diamond at normal temperatures and pressures. At 25 °C and 1 atmosphere, graphite is the stable polymorph of carbon, but for kinetic reasons the transition diamond → graphite does not occur at detectable rates under ambient conditions.

Since there is often no structural relationship between two polymorphs separated by a reconstructive phase transition, there may also be no relation between the symmetry and space groups of the two polymorphs.

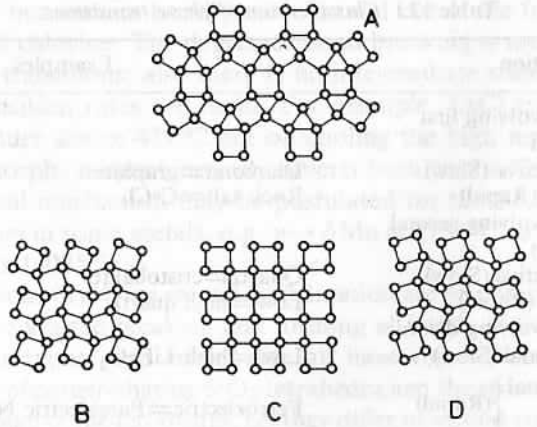

Fig. 12.1 Transformation from structure A to any other structure requires the breaking of first coordination bonds. Transformations among B, C and D are distortional only. (After Buerger, 1961)

Displacive phase transitions involve the distortion of bonds rather than their breaking and the structural changes that occur are usually small. For this reason, displacive transitions take place readily, with zero or small activation energies, and cannot usually be prevented from occurring. As well as a structural similarity, a symmetry relationship exists between the two polymorphs such that the symmetry of the low temperature polymorph is lower than, and belongs to a subgroup of, that of the high temperature polymorph. Examples are provided by the three main polymorphs of silica: quartz, tridymite and cristobalite, all of which undergo displacive, low–high transitions. These transitions involve small distortions or rotations of the SiO_4 tetrahedra, without breaking any primary Si—O bonds.

The distinction between reconstructive and displacive phase transitions is shown schematically in Fig. 12.1. In order to convert structure A into any of the other structures, B, C and D, bond breaking is necessary and the transition is reconstructive. On the other hand, interconversions between structures B, C and D do not involve bond breaking but only small rotational movements. These transitions are therefore displacive.

A more detailed and specific classification scheme, also due to Buerger, is given in Table 12.1. First coordination refers to bonds between nearest neighbour atoms (e.g. Si and O in SiO_4 tetrahedra), i.e. to the first coordination sphere of a particular atom. Second coordination refers to interactions between next nearest neighbour atoms (it is probably not true to regard these interactions as bonds), e.g. between adjacent silicon atoms in a chain of corner-sharing SiO_4 tetrahedra.

Transformations involving first coordination may occur by two mechanisms: (a) by completely disrupting the crystal structure of the original polymorph, as in graphite⇌diamond, or (b) by a much more subtle and easier method involving

Table 12.1 *Classification of phase transitions*

Type of transition	Examples
1. Transitions involving first coordination	
(a) Reconstructive (Slow)	Diamond⇌graphite
(b) Dilational (Rapid)	Rock salt⇌CsCl
2. Transitions involving second coordination	
(a) Reconstructive (Slow)	Quartz⇌cristobalite
(b) Displacive (Rapid)	Low⇌high quartz
3. Transitions involving disorder	
(a) Substitutional (Slow)	Low⇌high $LiFeO_2$
(b) Orientational / Rotational } (Rapid)	Ferroelectric⇌Paraelectric $NH_4H_2PO_4$
4. Transitions of bond type (Slow)	Grey⇌white Sn

dilation. An example of the latter is the rock salt⇌CsCl transition which occurs in several alkali and ammonium halides at high temperature and/or high pressure. Although the unit cell of rock salt is face centred cubic, $Z = 4$, a rhombohedral cell ($a = b = c, \alpha = \beta = \gamma = 60°$) that has one quarter the volume of the cubic cell, with $Z = 1$, can be defined (Fig. 5.16). The rhombohedral cell is primitive in that it has Na^+ ions at the corners and Cl^- at the body centre (or vice versa). If the rhombohedral cell is now compressed along its threefold axis, the angle α increases above 60° until, when $\alpha = 90°$, the structure has changed to that of CsCl (Fig. 12.2). The crystal structures of rock salt and CsCl are therefore interconvertible by this mechanism of dilation. A change in primary coordination number between 6 and 8 occurs. The bonds from chlorine to cations 2 to 7

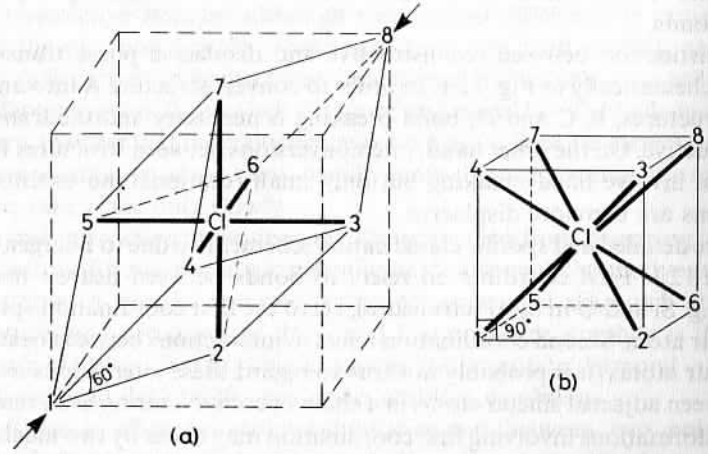

Fig. 12.2 Displacive phase transition between (a) rock salt and (b) CsCl structure types. Chlorine is octahedrally coordinate in (a) and eight-coordinate in (b). The cations are numbered 1 to 8

are unchanged but cations 1 and 8 move in and out of the first coordination environment of chlorine. The degree of bond breaking is much less than for reconstructive transitions; also there is no intermediate state of high energy and hence transition rates are rapid. For example, CsCl transforms to the rock salt structure above 479 °C but on cooling the high temperature, rock salt-like polymorph, it spontaneously reverts back to the CsCl structure. A similar dilational mechanism may be postulated for the f.c.c.→b.c.c. transition that occurs in some metals, e.g. $\gamma \rightarrow \delta$Mn at 1134 °C; $\alpha \rightarrow \gamma$Fe at 910 °C and $\gamma \rightarrow \delta$Fe at 1400 °C.

Transformations involving second coordination are reconstructive only if the mechanism involves the breaking and forming of bonds of first coordination. Thus quartz, tridymite and cristobalite all have three-dimensional network structures built of corner-sharing SiO_4 tetrahedra and the structures differ in the patterns of linkage of the tetrahedra, i.e. they differ in second coordination only. In order to transform from one polymorph to another, however, it is necessary to break and reform primary Si—O bonds.

Order–disorder transitions that involve atoms or ions exchanging places (i.e. substitutional effects) are usually sluggish. The structures of ordered and disordered polymorphs of $LiFeO_2$, stable below and above ~ 700 °C, respectively, are shown in Fig. 12.3. The disordered polymorph may be readily preserved to room temperature where it is kinetically stable. It has a rock salt structure with Li^+ and Fe^{3+} ions distributed at random over the octahedral sites of the face centred cubic unit cell (Fig. 12.3b). On heating disordered $LiFeO_2$ at, for example, 600 °C, the oxide ion arrangement remains unchanged but the cations order themselves over the octahedral sites (Fig. 12.3a), resulting in a larger unit cell of lower symmetry (tetragonal). The ordering reaction involves cation migration and takes place only slowly. As in all reconstructive tran-

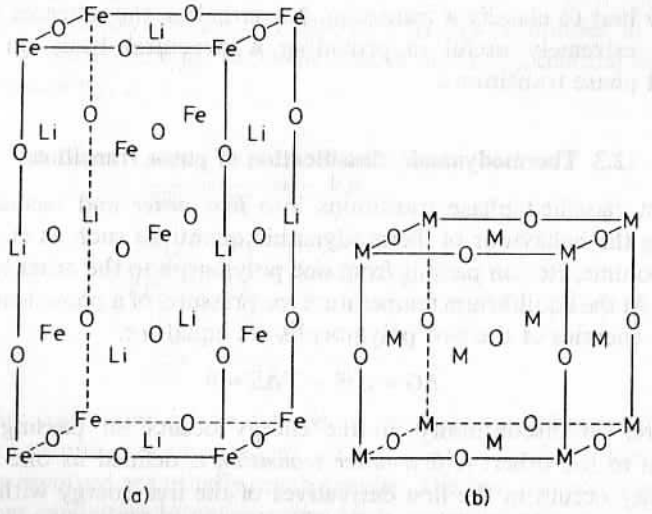

Fig. 12.3 (a) Ordered cation arrangement in tetragonal $LiFeO_2$; $a = 4.057$, $c = 8.759$ Å. (b) Disordered cation arrangement in cubic $LiFeO_2$ with the rock salt structure; a = ca. 4 Å; M = Li^+ or Fe^{3+}, at random

sitions, however, the transition rates are very temperature dependent. The ordering transition in $LiFeO_2$ is slow since 600 °C is, relatively, a low temperature. On the other hand, Li_2TiO_3 exhibits a similar order–disorder transition based on the rock salt structure, but since the equilibrium transition temperature is 1213 °C the ordering reaction in Li_2TiO_3 proceeds very rapidly on cooling below 1213 °C. Thus, the disordered polymorph of $LiFeO_2$ may be readily preserved to room temperature, but this is difficult to achieve with Li_2TiO_3.

A good example of an orientational order–disorder transition is the ferroelectric–paraelectric transition in $NH_4H_2PO_4$. Displacement of hydrogen atoms within —O—H—O— hydrogen bonds leads to an apparent change in the orientation of $PO_2(OH)_2$ tetrahedra (see Fig. 15.17). In the low temperature ferroelectric phase, these tetrahedra have a similar orientation, giving a net alignment of dipoles, but in the paraelectric phase they are randomized. Since the transition is accomplished by small displacements of hydrogen atoms, it takes place easily and rapidly.

The fourth category in Buerger's scheme involves transitions of bond type:

(a) grey⇌white tin, which involves a change from semiconducting to metallic character;
(b) diamond⇌graphite, which is insulting to semiconducting.

However, in addition to the change in bond type, major structural changes occur—in both tin and carbon, the primary coordination number changes at the transition—and hence these transitions could also be included in category 1(a).

In summary, the dividing lines between the different categories of phase transition, as classified by Buerger, are not rigid and in some cases it is difficult to decide how best to classify a transition. Nevertheless, the schemes of Buerger have been extremely useful in providing a structural basis on which to understand phase transitions.

12.3 Thermodynamic classification of phase transitions

Ehrenfest classified phase transitions into *first order* and *second order* by considering the behaviour of thermodynamic quantities such as entropy, heat capacity, volume, etc., on passing from one polymorph to the other through the transition. At the equilibrium temperature (or pressure) of a phase transition, the Gibbs free energies of the two polymorphs are equal: i.e.

$$\Delta G = \Delta H - T\Delta S = 0 \tag{12.1}$$

Therefore, no discontinuity in free energy occurs on passing from one polymorph to the other. A *first-order transition* is defined as one in which a discontinuity occurs in the first derivatives of the free energy with respect to temperature and pressure. These derivatives correspond to entropy and volume,

respectively, i.e.

$$\frac{dG}{dT} = -S \tag{12.2}$$

and

$$\frac{dG}{dP} = V \tag{12.3}$$

from

$$H = U + PV \tag{12.4}$$

Usually, first-order transitions are easy to detect. A discontinuity in volume corresponds to a change in crystal structure such that the density and the unit cell volume per formula unit are different in the two polymorphs. The change in volume may be followed by dilatometry (also called thermomechanical analysis) or sometimes by visual observation, e.g. the increase in volume associated with the tetragonal to monoclinic transition in ZrO_2 causes bodies containing tetragonal zirconia to shatter. Associated with a change in volume there is usually a change in enthalpy, ΔH (equation 12.4), which can be detected by DTA, Chapter 4; exothermic or endothermic peaks are observed as the transition proceeds. Direct measurement of entropy changes are less easily made but can also be inferred by the occurrence of DTA peaks; at the transition temperature, $\Delta G = 0$ and, therefore,

$$\Delta S = \frac{\Delta H}{T} \tag{12.5}$$

or by X-ray diffraction studies in the case of order–disorder transitions. Some examples of first-order phase transitions and their thermodynamic characteristics are given in Table 12.2.

Second-order transitions are characterized by discontinuities in the second derivatives of the free energy, i.e. in the heat capacity, C_p, thermal expansion, α, and compressibility, β:

$$\frac{\partial^2 G}{\partial P_T^2} = \frac{\partial V}{\partial P_T} = -V\beta \tag{12.6}$$

$$\frac{\partial^2 G}{\partial P \partial T} = \frac{\partial V}{\partial T_P} = V\alpha \tag{12.7}$$

$$\frac{\partial^2 G}{\partial T^2} = -\frac{\partial S}{\partial T_P} = \frac{-C_p}{T} \tag{12.8}$$

Higher order transitions can be defined, in principle, by differentiating further. Detection of second-order transitions is not so easy as for first-order ones since the changes involved are usually much smaller. The best method is probably to measure heat capacities, by calorimetry. Heat capacities usually increase as the

Table 12.2 *Characteristics of some first-order phase transitions.* (Taken in part from a compilation by Rao and Rao, 1966)

Compound	Transition	T_c(°C)	ΔV(cm^3)	ΔH(kJ mol^{-1})
Quartz, SiO_2	Low⇌high	573	1.33	0.360
CsCl	CsCl structure⇌rock salt structure	479	10.3	2.424
AgI	Wurtzite structure⇌b.c. cubic structure	145	−2.2	6.145
NH_4Cl	CsCl structure⇌rock salt structure	196	7.1	4.473
NH_4Br	CsCl structure⇌rock salt structure	179	9.5	3.678
Li_2SO_4	Monoclinic⇌cubic	590	3.81	28.842
$RbNO_3$	Trigonal structure⇌CsCl structure	166	6.0	3.971
	CsCl structure⇌hexagonal structure	228	3.12	2.717
	Hexagonal structure⇌NaCl structure	278	3.13	1.463

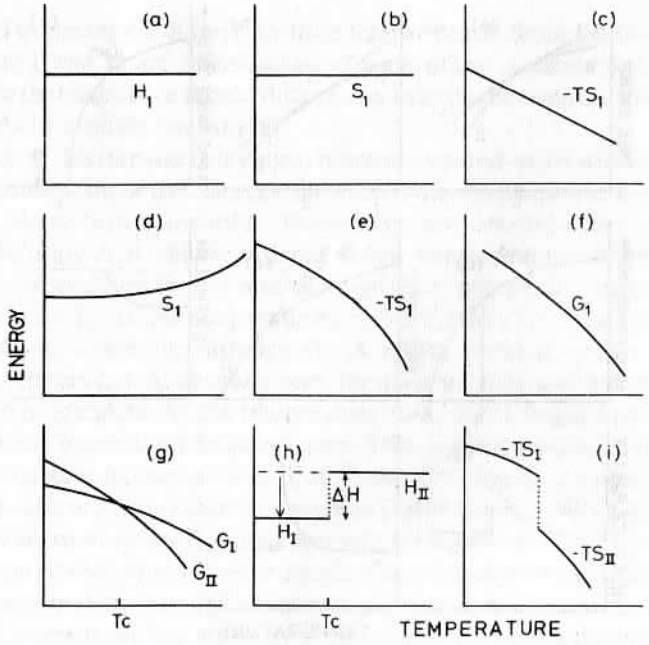

Fig. 12.4 (a) to (f) Thermodynamic properties of phases and (g) to (i) variations in these properties at first-order phase transitions

transition temperature, T_c, is approached and show a discontinuity at T_c (equation 12.8).

The temperature dependences of various thermodynamic functions in a polymorphic material are shown in Figs 12.4 and 12.5. In 12.4(a), the enthalpy H_1 of polymorph 1 is shown as being temperature independent, although in practice this is not strictly true. In Fig. 12.4(b), a temperature independent entropy S_1 is assumed which, again, is not strictly true in practice. This leads to a linear decrease in $-TS_1$ with increasing temperature (Fig. 12.4c). In Fig. 12.4(d), the entropy is shown as being markedly temperature dependent, especially at higher temperatures. This behaviour is characteristic of structures which experience some disorder with rising temperature. Consequently, $-TS_1$ decreases increasingly rapidly with rising temperature (Fig. 12.4e). For most materials, (a) and (e) are fairly good representations of their behaviour. These then give rise to a free energy that decreases increasingly rapidly with rising temperature (Fig. 12.4f).

In materials that are polymorphic, each polymorph has its own G–T curve, e.g. G_I and G_{II} (Fig. 12.4g); by definition, the polymorph that is stable under a particular set of conditions is the one of lower free energy, i.e. polymorph I at temperatures below T_c and polymorph II above T_c. The two curves cross over at the equilibrium transition temperature, T_c, at which $G_I = G_{II}$ (equation 12.1). The entropies of polymorphs I and II are given by the slopes of the G–T curves, i.e. $dG/dT = -S$. Hence, it follows that polymorph II has a higher entropy than

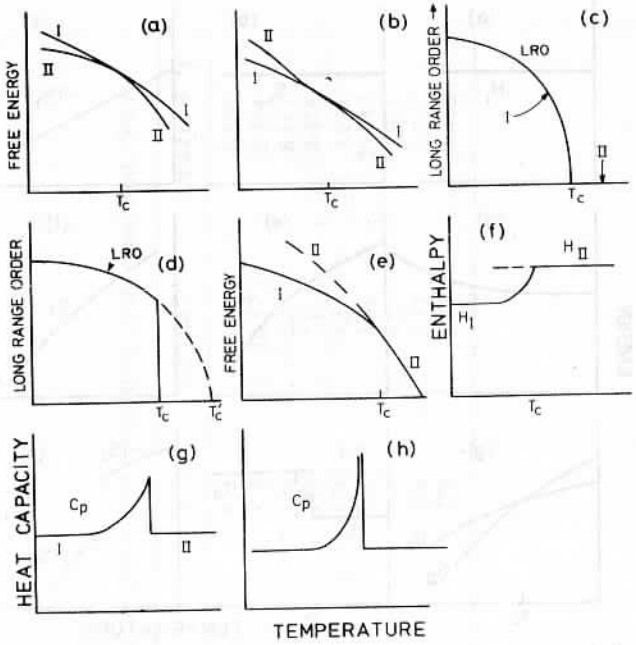

Fig. 12.5 Thermodynamic properties of phases involved in second-order phase transitions

polymorph I, i.e. $-TS_{II} < -TS_I$. From equation (12.5) polymorph II must also have a higher heat content than polymorph I, i.e. $H_I < H_{II}$. Broadly speaking, then, the polymorph which is stable at lower temperatures is the one with both the lower heat content and the lower entropy. Figures 12.4(h) and (i) show that discontinuities in H and S occur at T_c since although $\Delta G = 0$, $\Delta H = T\Delta S \neq 0$; these are the characteristics of a first-order phase transition. In order to get transformation from a low to a high temperature polymorph the latent heat of transformation, ΔH, must be provided. This explains a general principle of DTA that, on heating, transformation from one stable polymorph to another is endothermic and the reverse transition, on cooling, is exothermic (Chapter 4).

At a first-order transition, the G–T curves for the two polymorphs (Fig. 12.4g) intersect. This cannot be so for a second-order phase transition and the graphical and thermodynamic representation of second-order phase transitions presents some difficulties. Since, for a second-order transition, there is no discontinuity in entropy at T_c, the slope of the G–T curves ($dG/dT = -S$) for polymorphs I and II must be the same at T_c. Attempts to represent this graphically are shown in Fig. 12.5(a) and (b). Situation (a) is satisfactory from the point of view that the tangents to curves I and II at T_c are parallel and coincide (hence $\Delta S = S_{II} - S_I = 0$), but it is unsatisfactory because polymorph II always has the lower free energy and hence no reversible transition between I and II could ever be observed! This problem is partly overcome in Fig. 12.5(b), but at the cost of distorting the G–T curve of polymorph II and/or that of polymorph I so that they

are parallel in the region of the transition temperatures. Since the G–T curves of polymorphs I and II are independent of each other, it seems too much of a coincidence that one curve should distort over exactly the temperature range that corresponds to a phase transition.

A way out of this impasse in trying to represent second-order transitions comes from a consideration of the changes in thermodynamic properties for a practical example. Many order–disorder transitions are second-order transitions. Consider an alloy A_xB_y that is ordered at low temperatures but whose crystal structure is disordered (i.e. A and B atoms are placed at random) at high temperatures, $> T_c$. At low temperatures, below T_c, the alloy exhibits long range order (LRO) in which, for instance, the A atoms prefer a certain set of sites throughout the crystal. At absolute zero, the alloy must be perfectly ordered and hence LRO is complete. As the temperature rises, atoms begin to disorder and change places; hence the LRO decreases. This process continues increasingly rapidly as temperature increases until, at T_c, the LRO has disappeared altogether (Fig. 12.5c). Above T_c, only short range order (SRO) exists. In SRO, A atoms may prefer to be surrounded by B atoms, and vice versa, but this gives rise to regions that are ordered only on a very small scale. Disorder may be equated to entropy and it can be seen that, although an enormous increase in entropy occurs between 0 K and T_c, there is no discontinuity in entropy at T_c. Such a transition may be regarded as a second-order transition.

Consider now the form of the G–T curves for the ordered, I, and disordered, II, polymorphs in Fig. 12.5(c). These are shown schematically in Fig. 12.5(e). The dashed extension for curve II represents the disordered polymorph that has been supercooled to temperatures below T_c. However, it is impossible to do the reverse and superheat polymorph I above T_c because the process of continuous transition from I to II that begins at absolute zero has terminated at T_c. Temperature T_c represents the upper temperature limit of existence of I and, in this sense, it is a critical point, as, for example, the water–steam critical point. A thermodynamic theory due to Tizza treats phase transitions as critical points. The crucial difference between Fig. 12.5(e) and (b) is that, whereas it is possible to supercool II in both cases, it is impossible to superheat I in Fig. 12.5(e).

Thus far, the distinction between first order and second order transitions is clear cut and is based on thermodynamic principles. In practice, however, many transitions do not belong simply to one category or the other but may have hybrid character. This is illustrated graphically in Fig. 12.5(f). At some temperature well below T_c, there is a clear difference between the enthalpy of polymorph I, H_I and that of undercooled polymorph II, H_{II} (dashed line). On heating, the enthalpy of polymorph I shows a gradual, anomalous increase until, at temperature T_c, $H_I = H_{II}$. How are we to regard this transition? It is clearly not first order since at T_c, $H_I = H_{II}$. It may be possible to regard the change at T_c as a second order transition, especially if there is a discontinuity in C_p, as shown in Fig. 12.5(g). This is not very satisfactory, however since the classification of this transition as second order, based on its behaviour at T_c, ignores completely the large, anomalous increase in H_I below T_c.

A further way of classifying transitions which is both interesting and useful is that proposed by Ubbelohde. In this scheme, transitions are grouped into *continuous* and *discontinuous*. A continuous transition is one such as shown in Fig. 12.5(f): there is no discontinuity in enthalpy at T_c, but perhaps more importantly (and not shown), the crystal structure changes smoothly and continuously from that of polymorph I to that of polymorph II. A discontinuous transition is one such as quartz–cristobalite or diamond–graphite. In these, the structures of the two polymorphs are quite clearly different and it is not possible for the structure to change smoothly from one polymorph to the other.

Returning now to first and second order transitions, these represent extreme, ideal cases. Both are concerned only with the changes in thermodynamic properties at T_c. In practice, first order transitions usually show some 'premonitory' phenomena, such as an increase in disorder, as T_c is approached. However, such effects may be conveniently ignored, especially if there is a large change in enthalpy at T_c. In second order transitions, especially of the type order–disorder, almost all of the changes in structure and thermodynamic properties are associated with the 'premonitory' changes below T_c and surely cannot be ignored. For these, T_c merely represents the temperature at and above which the structural changes are complete.

In conclusion, then, most transitions, of whatever kind, show premonitory phenomena, which appear as an increase in heat capacity or a baseline drift on DTA, as T_c is approached (Fig. 12.5g). These premonitory phenomena may terminate with a discontinuity in e.g. enthalpy or LRO at T_c, in which case the transition is first order and discontinuous. Alternatively, if the transition did not take place with a discontinuity at T_c, then behaviour similar to that shown in Fig. 12.5(c) would be observed, with a continuous or second order transition at an extrapolated temperature T_c' (dashed line, Fig. 12.5d). We can see therefore, that premonitory phenomena, such as increasing disorder or defect concentrations, as T_c is approached, provide the link between first-order and second-order transitions. Premonitory phenomena also mark the onset of a continuous transition that may or may not be interrupted by a discontinuity.

A favourable philosophical point among physicists concerns the changeover from first-order to second-order behaviour: as a transition becomes increasingly second order in character, so the enthalpy of the transition at T_c decreases, but at what stage does this enthalpy become zero? Even though a transition has an extremely small ΔH, it must retain some first order character.

Many transitions that show finite or infinite discontinuities in C_p at T_c (Fig. 12.5g and h) are called *lambda transitions*, because the shape of the C_p curve resembles the Greek letter lambda. These are second-order transitions, if the change in C_p is finite (Fig. 12.5g), but are first order if ΔC_p is infinite (Fig. 12.5h). An example of a lambda transition is the low–high transition in quartz at 573 °C (Fig. 12.6). Changes in ΔH and ΔV occur at 573 °C, as given in Table 12.2, and therefore the transition has some first-order character. The rapid increase in C_p between ~500 and 573 °C shows the premonitory disordering effects that occur prior to the transition at T_c.

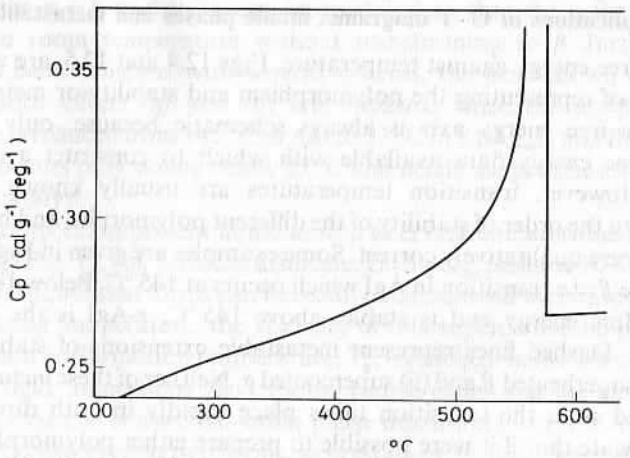

Fig. 12.6 Specific heat of crystalline quartz. (From Moser, 1936)

Most attention is given in this chapter to transitions that occur as a consequence of changing the temperature, but pressure-induced phase transitions also occur; some examples are given in Table 12.3. All of these transitions are accompanied by a decrease in volume and provide examples of the relevance of Le Chatelier's principle. In pressure-induced phase transitions, the effect of increased pressure is to cause a change in crystal structure such that the high pressure polymorph has a higher density and hence smaller volume than the low pressure polymorph. Schematic free energy–pressure diagrams may be constructed similar to the G–T relations given in Figs 12.4 and 12.5. For example, the C_p–T diagram in Fig. 12.5(g) would be replaced by a compressibility–P diagram.

The pressure dependence of phase transitions as a function of temperature is given by the *Clausius–Clapeyron equation*, which is a quantitative statement of Le Chatelier's principle:

$$\frac{dP}{dT} = \frac{\Delta H}{T\Delta V} \tag{12.9}$$

Table 12.3 *Some pressure-induced phase transitions.* (Data taken from Rao and Rao, 1966)

Compound	Transition	P_c(k bars)	$\Delta V(cm)^3$	ΔH(kJ mol^{-1})
KCl	Rock salt to CsCl structure	19.6	−4.11	8.03
KBr	Rock salt to CsCl structure	18.0	−4.17	7.65
RbCl	Rock salt to CsCl structure	5.7	−6.95	3.39
ZnO	Wurtzite to rock salt	88.6	−2.55	19.23
SiO_2	Quartz to coesite	18.8	−2.0	2.93
	Coesite to stishovite	93.1	−6.6	57.27
$CdTiO_3$	Ilmenite to perovskite	40.4	−2.9	15.88
$FeCr_2O_4$	Spinel to Cr_3S_4 structure	36.0	−6.5	−30.51

Transitions are at room temperature. P_c is the critical transformation pressure.

12.4 Applications of G–T diagrams; stable phases and metastable phases

Plots of free energy against temperature, Figs 12.4 and 12.5, are a useful and simple way of representing the polymorphism and stability or metastability of phases. The free energy axis is always schematic because, only rarely, are sufficient free energy data available with which to construct a quantitative diagram. However, transition temperatures are usually known accurately, together with the order of stability of the different polymorphs, and hence the *G–T* diagrams are qualitatively correct. Some examples are given in Fig. 12.7. In (a) is shown the $\beta \rightleftharpoons \alpha$ transition in AgI which occurs at 145 °C. Below 145 °C, β-AgI has lower free energy and is stable; above 145 °C, α-AgI is the equilibrium polymorph. Dashed lines represent metastable extensions of stable states; (i) represents superheated β and (ii) supercooled α. Neither of these *metastable* states is long-lived since the transition takes place rapidly in both directions. The arrows indicate that if it were possible to prepare either polymorph outside its range of stability, it would revert to the stable form, with a consequent decrease in free energy. This transition is important in the field of solid electrolytes. Much time has been spent studying doped AgI materials with the hope that either (a) the $\alpha \rightleftharpoons \beta$ transition temperature can be lowered so that the highly conducting α phase is stable to lower temperatures, especially to room temperature, or (b) the

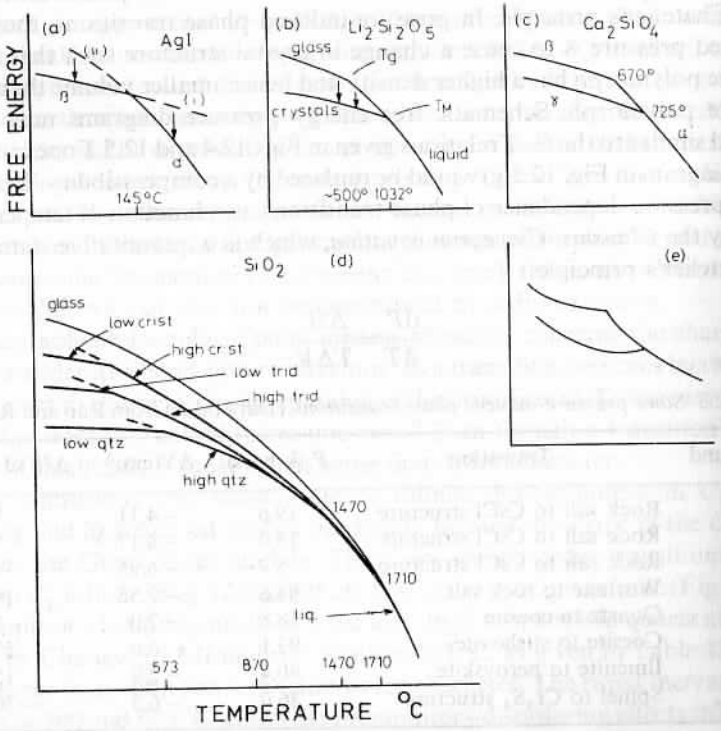

Fig. 12.7 Free energy–temperature diagrams showing polymorphism

kinetics of the $\alpha \rightarrow \beta$ transition can be modified so that the α form could be quenched to room temperature without transforming to β during cooling. Success has been achieved with several systems, the best known of which is $RbAg_4I_5$. Both effects (a) and (b) are observed since the $\alpha \rightleftharpoons \beta$ transition temperature is reduced from 145 °C in AgI to 27 °C in $RbAg_4I_5$ and the transition from α to β occurs only slowly below 27 °C and needs the presence of free iodine to act as a catalyst.

G–T diagrams can represent liquid as well as crystalline substances, as shown for $Li_2Si_2O_5$ (Fig. 12.7b). Lithium disilicate, $Li_2Si_2O_5$, melts at 1032 °C and the rather viscous liquid that forms can be readily undercooled without crystallizing. With decreasing temperature, the viscosity of this supercooled liquid increases until the glass transformation temperature, T_g, is reached, below which the liquid freezes to a rigid, amorphous glass. (Some people claim that the glass transformation is an example of a second-order phase transition.) At room temperature, then, $Li_2Si_2O_5$ can exist in two forms, as crystals or as glass. Since the glass has higher free energy it is metastable and will crystallize, provided the conditions are kinetically favourable. This metastability of glass, and its subsequent crystallization on heating at high temperatures (~ 450 to 700 °C), forms the basis of the manufacture of glass-ceramics (pyrosil, pyroceram, slagceram, etc.). Glass-ceramics withstand high temperatures, unlike most glasses which soften or crystallize, and are resistant to thermal shock (see Chapter 18). Figure 12.7(b) is somewhat simplified in that crystalline $Li_2Si_2O_5$ undergoes minor polymorphic phase transitions at ~970°C, but these have been omitted for clarity.

Examples of phase transitions that must be avoided if possible are the $\alpha' \rightarrow \gamma$ and $\beta \rightarrow \gamma$ transitions in Ca_2SiO_4, which is present as a major constituent of cement. Under equilibrium conditions, the α' polymorph of Ca_2SiO_4 should transform to γ below 725 °C (Fig. 12.7c). However, with rapid cooling and/or the addition of suitable additives, the $\alpha' \rightarrow \gamma$ transition does not occur and, instead, undercooled α' transforms to β below 670 °C. β-Ca_2SiO_4 is entirely metastable since at all temperatures over which it can exist it has a higher free energy than γ-Ca_2SiO_4. β-Ca_2SiO_4 is one of the major components of Portland cement clinker and it sets hard on reaction with water. On the other hand γ-Ca_2SiO_4 has very little cementitious value and, hence, in the manufacture of Portland cement, transformation to give the γ polymorph must be avoided.

A material with a complex *G–T* diagram is silica, SiO_2. The equilibrium forms, as a function of temperature, are:

$$\text{Low quartz} \overset{573\,^\circ C}{\rightleftharpoons} \text{high quartz} \overset{870\,^\circ C}{\rightleftharpoons} \text{high tridymite} \overset{1470\,^\circ C}{\rightleftharpoons}$$
$$\text{high cristobalite} \overset{1710\,^\circ C}{\rightleftharpoons} \text{liquid}$$

The three main crystalline polymorphs, quartz, tridymite and cristobalite, all undergo high→low transitions on cooling, but both low tridymite and low cristobalite are entirely metastable relative to low quartz (Fig. 12.7d). Once formed, however, both tridymite and cristobalite are kinetically stable outside

their ranges of equilibrium existence (i.e. below 870 and 1470 °C, respectively) and their subsequent conversion to quartz on lowering the temperature proceeds only slowly because these transitions are reconstructive. Silica glass can be prepared by supercooling silica liquid. The glass transformation temperature, T_g, is high, ~1200 °C. Silica also forms high pressure polymorphs, coesite and stishovite, but these do not appear on Fig. 12.7(d).

With complex G–T diagrams, such as Fig. 12.7(d), it is often difficult to show the transition points clearly. In order to make the drawings clearer, some authors use diagrams such as Fig. 12.7(e) in which each G–T curve is shown as being concave upwards, rather than concave downwards as in Fig. 12.7(d). While the drawings are certainly clearer, they are thermodynamically incorrect and their use is not to be encouraged. For instance, the G–T curve for each polymorph must become horizontal as absolute zero is approached since $\mathrm{d}G/\mathrm{d}T = -S$ and $S \rightarrow 0$ at 0 K. Figure 12.7(e) shows the opposite of this.

All the examples considered in Fig. 12.7 are for one-component systems in which all polymorphs have the same composition. Similar representations can be used for multicomponent systems although it becomes more difficult to show the effect of three variables—G, T, composition—on a single diagram. One application in multicomponent systems is in the phenomenon of spinodal decomposition, which is an important effect associated with liquid immiscibility (Chapter 18).

DTA may be used in favourable circumstances to distinguish between phases that are stable and metastable. The change from one stable polymorph to another on heating should appear on DTA as an endothermic event. The change from a quenched, metastable polymorph to a stable polymorph on heating should appear as an exothermic event. An example would be the crystallization of $Li_2Si_2O_5$ glass on heating; crystallization would occur at ~600 to 800 °C and give an exotherm on DTA (Fig. 4.7b).

12.5 Ubbelohde's classification: continuous and discountinuous transitions

As mentioned in the previous section separation of phase transitions into first order and second order according to thermodynamic principles is fine in theory but does not work so well in practice because many transitions have an intermediate character. An alternative scheme, due to Ubbelohde (1957), classifies transitions into two groups, *continuous* and *discontinuous*. Broadly speaking, discontinuous and continuous transitions correspond to thermodynamic first- and second-order transitions, respectively. Ubbelohde's scheme has been particularly useful for transitions that experimentally involve only minor structural changes. In many cases, these transitions proceed by the formation of 'hybrid crystals' in which domains of the product phase grow inside the parent crystal. At the interface between parent and product crystals, one or both phases will be in a stressed condition since it is unlikely that the molar volume of the two phases is identical. The free energies of the two phases are therefore modified by a strain energy term ξ and this leads to a modified phase rule in which the strain energy contributes an extra degree of freedom:

$$P + F = C + 2 + \sum \pi$$

where $\sum \pi$ refers to the number of additional degrees of freedom introduced (as well as strain energy, surface energy may also be important, there by contributing a further degree of freedom). Some transitions have been studied directly by high temperature single crystal X-ray diffraction and the presence of hybrid crystals observed over a range of temperatures. Using the modified phase rule, these observations may be rationalized and it is not necessary to invoke any violations of the phase rule. It seems highly probable that there is a close relation between the occurrence of hybrid crystals and the phenomenon of martensitic transformations (Section 12.8.2).

12.6 Representation of phase transitions on phase diagrams

Phase diagrams are treated systematically in Chapter 11. Some further points regarding the representation of phase transitions on phase diagrams are worth making here:

(a) In one-component systems, e.g. C, SiO_2, which are subjected to changes in temperature and pressure, first-order phase transitions represent univariant conditions. From the phase rule, for a one-component system, $P + F = C + 2 = 3$. At the transition point, two phases are in equilibrium, $P = 2$ and so $F = 1$. The transition temperature therefore changes if the pressure is varied, and vice versa, e.g. Figs 11.3, 11.4 and 11.5. The condensed phase rule, $P + F = C + 1$, is used in condensed systems where the vapour phase is unimportant and for transitions that take place at fixed (often ambient) pressure. In such cases, first-order transitions occur at fixed temperatures, i.e. at invariant points.

(b) In two-component solid solution systems that exhibit phase transitions, addition of the extra component, composition, generates, from the phase rule, an extra degree of freedom. Whereas two phases coexist at a fixed point in a condensed, one-component system, two phases may coexist over a range of temperatures in a binary solid solution (Fig. 11.18a). These two phase regions, such as $\alpha + \beta$, must be present in theory, although in practice they are sometimes narrow and difficult to detect.

(c) Second-order phase transitions, strictly speaking, cannot be represented on equilibrium phase diagrams. In a second-order or continuous transition, the critical temperature represents the condition under which the low–high transition is complete. At no stage do two phases coexist in equilibrium. Since $P = 1$ throughout, it is impossible to represent a second-order phase transition on a conventional phase diagram because the latter demands that, at a transition point, $P = 2$. It is necessary, of course, to be able to represent such phase transitions and this may be done by using a single curve to

represent the variation of transition temperature with, for example, composition.

12.7 Kinetics of phase transitions

Thermodynamics tells us the temperature (and pressure) at which a transition occurs under equilibrium conditions but gives no information about the rates at which transitions occur. The latter is the subject of kinetics. The rates at which transitions occur vary enormously. At one extreme are transitions that take place very rapidly in both forward and back directions and without any hysteresis (i.e. the transition temperature is the same on heating and cooling). At the other extreme are transitions that occur only on geological timescales; e.g. obsidian, a glassy mineral, should transform to one of the crystalline forms of SiO_2 but clearly, from the occurrence of obsidian as a mineral, the transition rates are very slow. Most transitions are intermediate between these extremes and occur with some hysteresis, i.e. the high temperature polymorph may be undercooled to varying degrees before transforming to the low temperature polymorph.

Transition rates vary enormously and are controlled by several factors. In Fig. 12.8 the temperature dependence of the rate of transition between a low temperature polymorph, I, and a high temperature polymorph, II, is shown schematically. Rates are slow in either direction at temperatures that are close to the equilibrium transition temperature, T_c (region A). Since $\Delta G \sim 0$ close to T_c, there is little driving force for the transition to occur in either direction. At temperatures further removed from T_c, reaction rates increase (regions B, C). A maximum in the rate of the II → I transition may occur at a certain degree of undercooling, at T_M, and if it is possible to undercool the high form II to below T_M then the rate of the II → I transition again decreases (region D). If the maximum

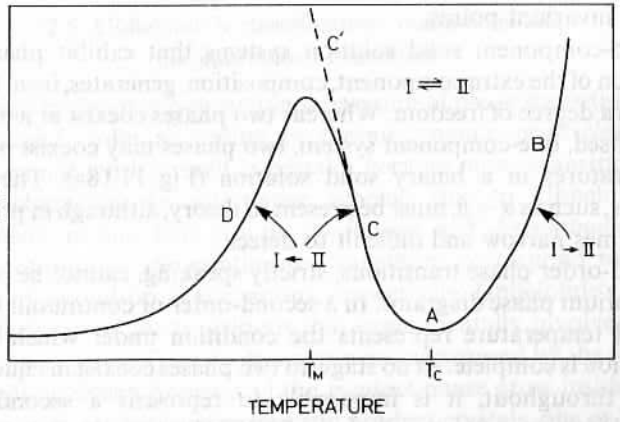

Fig. 12.8 Temperature dependence of the transition rates for a typical first-order transition between a low temperature polymorph, I, and a high temperature polymorph, II

cannot be detected experimentally, then the II → I transition rate continues to increase (region C'), although, in theory, a maximum may still occur at some lower temperature. There is no corresponding maximum in the I → II transition above T_c; instead the rate increases increasingly rapidly (region B).

The general form of Fig. 12.8 and the occurrence of the maximum at T_M may be understood by considering the combination of (a) the effect of temperature on reaction rates, as given by the Arrhenius equation and (b) the relative free energies of the polymorphs I and II as a function of temperature. These two effects are as follows:

(a) The Arrhenius equation, as applied to kinetics, is of the form:

$$\text{Rate} = A \exp\left(\frac{-E}{RT}\right) \tag{12.10}$$

where E is the activation energy of the transition. This equation predicts a rapid increase in rate with increasing temperature, as observed in regions D and B of Fig. 12.8. The usual method of analysing results in terms of the Arrhenius equation is, of course, to take logs:

$$\log_{10}\text{rate} = \log_{10}A - \frac{E}{RT}\log_{10}e \tag{12.11}$$

and plot $\log_{10}$ rate against $1/T$. If the data fit the Arrhenius equation, a straight line is obtained of slope $(-E/R)\log_{10}e$ and intercept (extrapolated) equal to $\log_{10}A$.

(b) The magnitude of the difference in free energy $\Delta G_{I\text{-}II}$ between the two polymorphs I and II gives a measure of the driving force for the transition to occur (Fig. 12.9). At T_c, $G_I = G_{II}$ and there is no driving force for the transition to occur in either direction (Fig. 12.9a). At any other temperature, $G_I \neq G_{II}$ and the transition takes place preferentially in one direction (Fig. 12.9b). For idealized transitions in which H and S of the two polymorphs are independent of temperature (Fig. 12.4a and b), the magni-

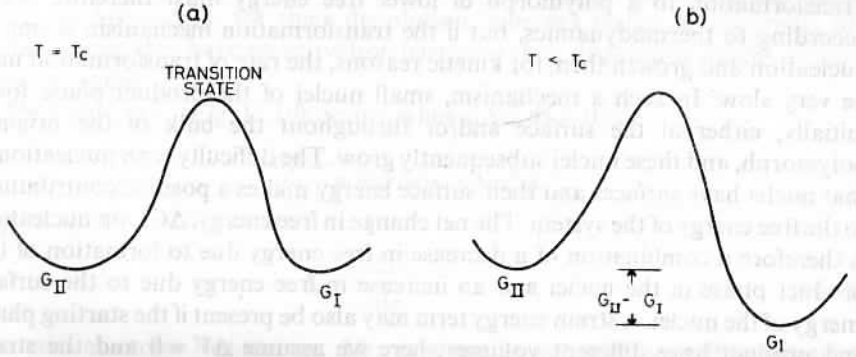

Fig. 12.9 Difference in free energy between polymorphs I and II

tude of ΔG_{I-II} at temperature T is a simple function of the difference in temperature $(T_e - T)$:

$$\Delta G_{I-II} = \Delta H_{I-II} - T\Delta S_{I-II} \quad (12.12)$$

$$= (T_e - T)\Delta S_{I-II} \quad (12.13)$$

or

$$\Delta G_{I-II} = \frac{T_e - T}{T}\Delta H_{I-II} \quad (12.14)$$

Both factors (a) and (b) outlined above are important in controlling the rates at which phase transitions occur. Qualitatively, factor (b) is dominant at temperatures close to T_e where there is little thermodynamic driving force for the transition to occur. At temperatures further away from T_e, however, factor (a) becomes more important, especially in regions D and B of Fig. 12.8, where the transition rate increases increasingly rapidly with rising temperature.

Difficulties arise when attempts are made to quantify the effects of factor (a) and, especially, factor (b). The traditional approach is to relate the thermodynamic driving force, given by ΔG_{I-II}, factor (b), to the problem of forming nuclei of the product phase. Most first-order or reconstructive transitions take place by a mechanism of *nucleation and growth*, in which the slow step is the initial nucleation of the product phase. Although the theory of nucleation is well developed, it is difficult, if not impossible, to apply it quantitatively since the magnitudes of certain parameters, such as the surface energies of nuclei, are not known. This theory is now briefly described.

12.7.1 Critical size of nuclei

Let us begin with a phase which is in its field of thermodynamic stability. Transformation or reaction to give another polymorph cannot occur to any appreciable extent, because this would lead to an overall increase in free energy (e.g. transformation in the direction I → II in Fig. 12.9b).

Suppose now that the conditions, T or P, of the original polymorph are changed so that it moves outside its field of equilibrium existence. Transformation to a polymorph of lower free energy must therefore occur according to thermodynamics, but if the transformation mechanism is one of nucleation and growth then, for kinetic reasons, the rate of transformation may be very slow. In such a mechanism, small nuclei of the product phase form initially, either at the surface and/or throughout the bulk of the original polymorph, and these nuclei subsequently grow. The difficulty with nucleation is that nuclei have surfaces and their surface energy makes a positive contribution to the free energy of the system. The net change in free energy, ΔG_n, on nucleation is therefore a combination of a decrease in free energy due to formation of the product phase in the nuclei and an increase in free energy due to the surface energy of the nuclei. A strain energy term may also be present if the starting phase and product have different volumes; here we assume $\Delta V = 0$ and the strain

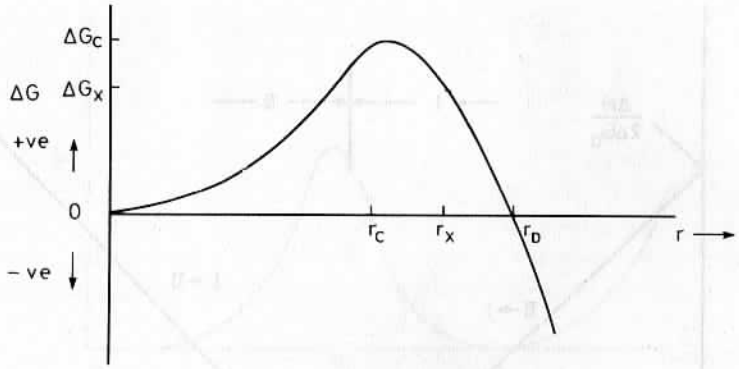

Fig. 12.10 Change in free energy of nuclei as a function of raduis

energy is zero. Let us assume that ΔG_v represents the free energy per unit volume of the nucleus relative to the parent phase and ΔG_a represents the surface free energy per unit area of the nucleus. For a spherical nucleus of radius r,

$$\Delta G_n = 4\pi r^2 \Delta G_a - \tfrac{4}{3}\pi r^3 \Delta G_v \quad (12.15)$$

For small values of r, ΔG_n is positive since $4\pi r^2 \Delta G_a > \frac{4}{3}\pi r^3 \Delta G_v$ (Fig. 12.10), but with increasing r, ΔG_n passes through a maximum ΔG_c at $r = r_c$, and decreases to zero at $r = r_D$. For $r > r_D$, ΔG_n is negative. This then gives rise to the notion that a nucleus should have a certain minimum size in order for it to be stable. At first sight, it might be thought that r_D represents the critical radius of the nucleus, above which the nucleus is stable because ΔG_n is negative. Kinetically, however, the critical radius corresponds to r_c since for $r > r_c$, ΔG_n decreases with increasing r. In order to understand this, consider a nucleus of intermediate radius, r_X and free energy $+\Delta G_X$. While such a nucleus is unstable thermodynamically, it is stable kinetically since, if it were to start dissolving, r would decrease and the free energy would begin to rise towards the value ΔG_c. Once nuclei of size $r > r_c$ form, therefore, they are kinetically stable and continue to grow. In fact, nuclei of radius r_X, where $r_c < r_X < r_D$, are *metastable* since they require an activation energy, given by $\Delta G_c - \Delta G_X$, for their dissolution, whereas nuclei of size $r < r_c$ are *unstable* since they have no activation barrier to their dissolution; nuclei of size $r > r_D$ are *stable*.

The value of r_c (Fig. 12.10) occurs when $d\Delta G/dr = 0$; i.e.

$$\frac{d\Delta G}{dr} = 8\pi r \Delta G_a - 4\pi r^2 \Delta G_v$$

and

$$r_c = \frac{2\Delta G_a}{\Delta G_v} \quad (12.16)$$

The critical excess free energy, ΔG_c, is given by substituting r_c into equation

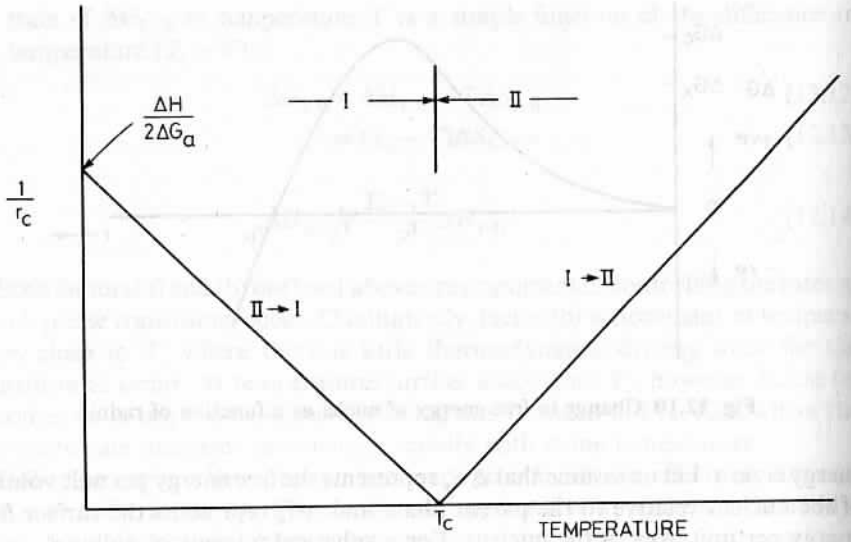

Fig. 12.11 Critical size of nuclei as a function of temperature

(12.15), i.e.

$$\Delta G_c = \frac{16}{3}\frac{\pi \Delta G_a^3}{\Delta G_v^2} \tag{12.17}$$

We can now see why nucleation is difficult at temperatures close to T_c. Since $\Delta G_v \rightarrow 0$ as $T \rightarrow T_c$ then, from equations (12.16) and (12.17), both r_c and ΔG_c become increasingly large as T_c is approached. The variation of r_c with temperature is given by substituting equation (12.14) into (12.16), i.e.

$$r_c = \frac{2\Delta G_a T_c}{(T_c - T)\Delta H} \tag{12.18}$$

A plot of r_c^{-1} against T (Fig. 12.11) should be linear, intersecting the T axis at T_c as $r \rightarrow \infty$. The two lines on Fig. 12.11 correspond to the two transformation directions, I⇌II.

12.7.2 Rate equations

12.7.2.1 *Nucleation rate*

Nuclei of the product phase form as a consequence of the thermal motion of atoms; the rate of nucleation is given by

$$R = A \exp\left[\frac{-(\Delta G_c + \Delta G_a)}{kT}\right] \tag{12.19}$$

The overall activation energy, $\Delta G_c + \Delta G_a$, is a combination of the critical free

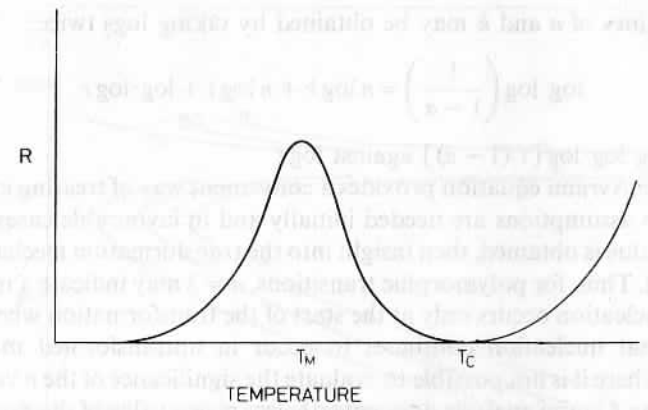

Fig. 12.12 Effect of temperature on nucleation rate, R

energy, ΔG_c, which must be surmounted in order for the nuclei to be stable and the activation energy, ΔG_a, for the individual atomic jumps involved in nucleation. Since ΔG_c is temperature dependent, equations (12.17) and (12.14), the nucleation rate, R, varies with temperature as shown in Fig. 12.12. For transformation in the direction II → I, R passes through a maximum at a certain temperature T_M, below T_c, and tends to zero both at 0 K and at T_c. For transformation in the direction I → II, R increases rapidly with temperature above T_c.

There is considerable evidence that equation (12.19) and Fig. 12.12 represent, at least qualitatively, the kinetics of nucleation in many transitions. However, it is difficult to measure nucleation rates experimentally and test the theories. Part of the difficulty is that nucleation is very dependent on the presence of impurities, dislocations, surfaces, etc. It is possible to distinguish two types of nucleation. *Homogeneous nucleation* occurs when all parts of the parent phase are identical. This is a random process and depends only on thermal fluctuations in atomic positions. Usually, however, it is much easier for *heterogeneous nucleation* to occur in which nucleation takes place preferentially at defect centres and sites of higher local free energy.

12.7.2.2 *Overall transformation rate—Avrami equation*

Experimentally, it is much easier to measure the overall rate of transformation than to try and isolate the nucleation and growth stages, especially if the substance under study is a powder. Many data are analysed using the Avrami equation (also called the Avrami–Johnson–Mehl–Erofeev equation):

$$\alpha = 1 - \exp(-kt)^n \tag{12.20}$$

in which α is the volume fraction of the product phase, k is the rate constant and n is a constant whose value depends on the nature of the nucleation and growth

process. Values of n and k may be obtained by taking logs twice:

$$\log\cdot\log\left(\frac{1}{1-\alpha}\right) = n\log k + n\log t + \log\cdot\log e \qquad (12.21)$$

and plotting $\log\cdot\log[1/(1-\alpha)]$ against $\log t$.

Use of the Avrami equation provides a convenient way of treating experimental data; no assumptions are needed initially and in favourable cases, e.g. if an integral n value is obtained, then insight into the transformation mechanism may be obtained. Thus, for polymorphic transitions, $n = 3$ may indicate a mechanism in which nucleation occurs only at the start of the transformation whereas $n = 4$ indicates that nucleation continues to occur in untransformed material. In situations where it is not possible to evaluate the significance of the n value that is obtained, the Avrami analysis does nevertheless give a value of the rate constant parameter k. If measurements on the transformation rate are made over a range of temperatures, an activation energy may then be obtained from an Arrhenius plot of $\log k$ against T^{-1}. An example is shown in Fig. 12.13 for the polymorphic transition $\beta \rightleftharpoons \gamma$ in Li_2ZnSiO_4. The kinetics were studied over a large temperature range, 480 to 940 °C, and in both transformation directions. At temperatures well below T_c, 883 °C, the data fall on a straight line and give an activation energy of 185 kJ mol^{-1}. Between 780 and 950 °C, however, the transformation rates are reduced, especially in the region of T_c. This result serves to emphasize the importance of thermodynamic factors, i.e. the relative free energies of the two polymorphs, to the kinetics of phase transitions.

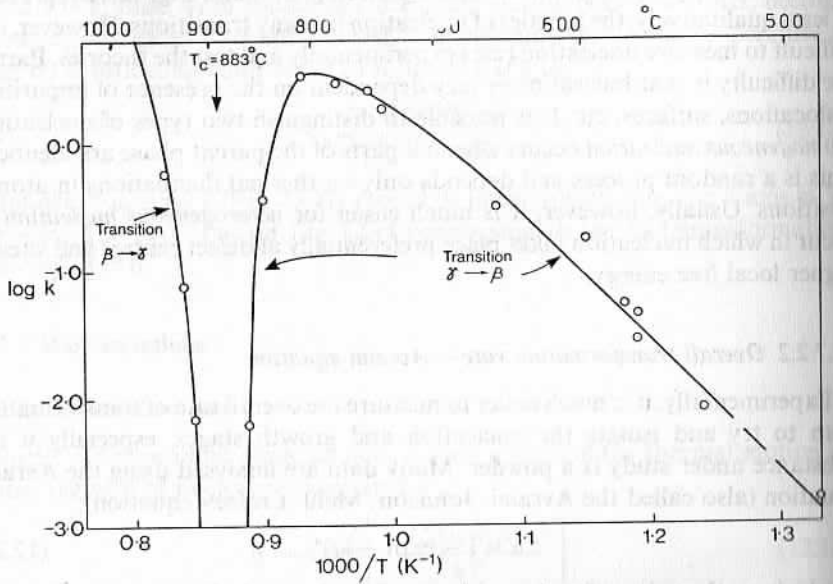

Fig. 12.13 Arrhenius plot for the rate of transition $\beta \rightleftharpoons \gamma$ in Li_2ZnSiO_4. (Data from Villafuerte-Castrejon and West, 1981)

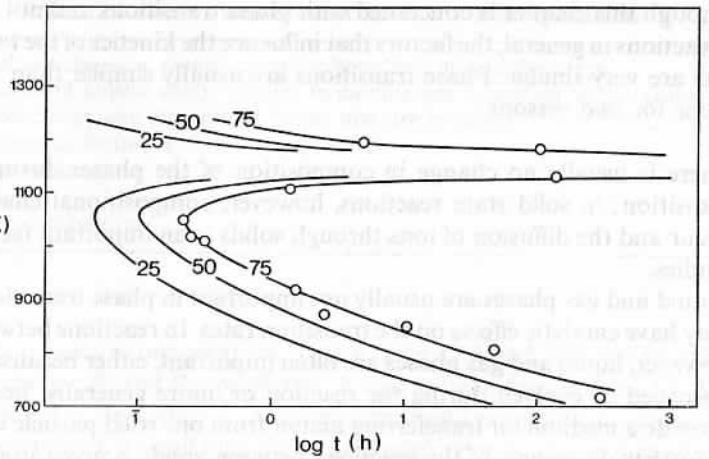

Fig. 12.14 Time–temperature–transformation (TTT) diagram for the transition $\beta \rightleftharpoons \gamma$ in Li_2ZnSiO_4

12.7.2.3 *Time–temperature–transformation (TTT) diagrams*

In experimental studies on phase transitions, one is often interested in a general knowledge of reaction rates as a function of temperature without being particularly concerned with details of the mechanism or the correct rate equation to use. It is then convenient to plot kinetic data as TTT diagrams, in which the time taken to achieve a certain degree of conversion, say 25 per cent, is ascertained over a range of temperatures; a graph of temperature against log time is constructed. As an example, data for the $\beta \rightleftharpoons \gamma$ transition in Li_2ZnSiO_4 (Fig. 12.13) are replotted as a TTT diagram (Fig. 12.14) for 25, 50 and 75 per cent conversion. The graphs show that transition rates for the $\gamma \rightarrow \beta$ direction pass through a maximum at ~ 1060 K (i.e. ~ 790 °C) and that at ~ 1150 K, transition rates are extremely slow in either direction. A rapid increase in the rate of $\beta \rightarrow \gamma$ transition occurs above ~ 1180 K.

TTT curves similar to Fig. 12.14 have been observed in many metals and alloys. They are probably characteristic of many inorganic phase transitions as well.

12.7.3 Factors that influence the kinetics of phase transitions

In most books on kinetics, attention is focused on reactions in the gaseous and liquid states with barely a mention of solids, apart from the use of solids to catalyse liquid and/or gaseous reactions. The reason for this is not that reactions involving solids are unimportant—they obviously are extremely important—but that solid state reactions are highly complex; rigorous, quantitative interpretation of the results of such reactions is difficult, if not impossible. For example, the concept of reaction order, which is a central, indispensable feature of the study of gaseous reactions, is meaningless in most solid reactions.

Although this chapter is concerned with phase transitions and not with solid state reactions in general, the factors that influence the kinetics of the two types of process are very similar. Phase transitions are usually simpler than solid state reactions for two reasons:

(a) There is usually no change in composition of the phases during a phase transition; in solid state reactions, however, compositional changes must occur and the diffusion of ions through solids is an important factor in rate studies.
(b) Liquid and gas phases are usually not important in phase transitions, unless they have catalytic effects on the transition rates. In reactions between solids, however, liquid and gas phases are often important, either because gases are absorbed or evolved during the reaction or, more generally, because they provide a medium for transferring matter from one solid particle to another. A further discussion of the reactions between solids is given in Chapter 2.

Comparison of the kinetics and mechanism of phase transitions, on the one hand, and reactions involving liquid or gas phases, on the other, shows that there are major differences between them. The most striking difference is one of scale. Liquid and gas reactions involve only a small number of atoms in each self-contained reaction, e.g. reaction of a hydrogen atom and a chlorine atom to form a molecule of hydrogen chloride:

$$H + \cdot Cl \rightarrow HCl$$

In most phase transitions, however, a much larger number of atoms are involved in forming a stable nucleus of the product phase. For example, in the transformation of anatase, TiO_2, to rutile, nuclei of rutile form both at the surface and throughout the bulk of the anatase crystals and these nuclei grow with increasing time. Let us suppose that under a certain set of conditions, the smallest nucleus of rutile capable of independent existence has a diameter of 50 Å. Such a nucleus contains about 5000 atoms!

Another difference between gas and solid reactions is that the latter are strongly influenced by surface effects: nucleation of the product phase often occurs at sites on the surface of the original crystals. The transformation kinetics depend on the total surface area of the original crystals, therefore, and on whether, for example, a single crystal or a powdered sample is used. Surface effects also control whether or not a nucleus of the product phase is stable, as discussed above. The surface energy of a nucleus gives a positive contribution to the free energy and if this more than cancels the decrease in free energy in the bulk of the nuclei, then such nuclei are unstable and redissolve. In contrast, surfaces are unimportant in gas and liquid reactions unless the reactions occur with the aid of solid catalysts.

Many other factors influence the kinetics of phase transitions, some of which are summarized in Table 12.4. The surface area of the sample has already been mentioned as well as the effect of the temperature of study relative to the

Table 12.4 *Factors that influence kinetics of phase transitions*

1. Nature of sample—e.g. single crystal or powder—and surface area
2. Temperature of kinetic study, relative to equilibrium transition temperature
3. Activation energy and strength of bonds that are broken
4. Pre-exponential factor, A
5. Change in volume, ΔV
6. Pressure, P
7. Transition mechanism

equilibrium transition temperature, T_c (e.g. Figs 12.8 and 12.13). The effect of activation energy, E, and the prefactor, A, can be seen from Fig. 12.13. A high value of A ($\log A = \log k$ when $T^{-1} \rightarrow 0$) ensures rapid rates at high temperatures. If, at the same time, E is small then these rapid rates extend to lower temperatures. The value of E gives a measure of the strengths of the bonds that are broken in order to form the transition state. Hence, major reconstructive transitions have large E values and are slow whereas minor displacive transitions have much smaller E values and are rapid.

Transition rates also depend on the difference in volume, ΔV, between the two polymorphs. From absolute reaction rate theory,

$$\log(\text{rate}) = \text{constant} - \frac{\Delta V^* P}{RT} \qquad (12.22)$$

where ΔV^* is the difference in volume between the initial polymorph and the transition state.

It can be seen that the rate decreases with increasing ΔV. Many transitions are accomplished under high pressure and equation (12.22) shows that the reaction rate also decreases with increasing pressure. This has consequences in, for example, the synthesis of diamond from graphite. Diamond is thermodynamically stable only at high pressures. The effect of increasing pressure is to increase its stability, but at the same time its rate of formation in reduced.

The mechanism of transition is a major factor that effects the transition rates, e.g. compare dilational and reconstructive transition mechanisms in Table 12.1. Nucleation is the rate limiting step in many transitions and depends on many factors, including the nature of the solid (i.e. single crystal or powder), crystal defects (i.e. vacancies, dislocations, impurities, etc.) and atmosphere. The difference in crystal structure between the two polymorphs also greatly affects the ease of nucleation. If the structural differences are small and involve changes in second coordination only, then nucleation is very easy. At the other extreme, if there is no structural similarity between the two phases, nucleation is difficult. An intermediate class of transitions are *topotactic transitions* in which a definite orientation relation exists between the two phases but in which, nevertheless, considerable structural reorganization is necessary. Examples include transitions

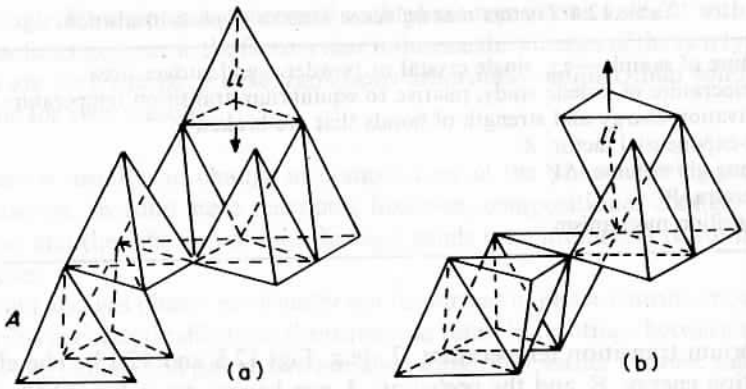

Fig. 12.15 Topotactic mechanism for the transformation $\beta \rightleftharpoons \gamma$ in Li_2ZnSiO_4. (From West, 1975)

in which the anion arrangement is unchanged throughout the transition but cation reorganization occurs. In such cases, nucleation is moderately difficult. A topotactic mechanism has been proposed for the transition $\beta \rightleftharpoons \gamma$ in Li_2ZnSiO_4 (Fig. 12.15). β-Li_2ZnSiO_4 has a wurtzite derivative structure with the cations ordered over one set of tetrahedral sites in a hexagonal close packed oxide array. On transformation to γ-Li_2ZnSiO_4 the oxygen layers are unchanged apart from a slight buckling, but half the cations move from filled to empty tetrahedral sites. This is represented by inversion of some of the MO_4 tetrahedra in Fig. 12.15.

An additional factor that is well appreciated in gas phase reactions and is likely to be important also in solid state reactions and transitions is the *principle of microscopic reversibility*. This states that, for a reaction that may be represented simply by

$$A \underset{k_{-1}}{\overset{k_1}{\rightleftharpoons}} B$$

both forward and back reactions occur, with rate constants k_1 and k_{-1}. In the gas phase reactions, this has two consequences. First, the overall rate constant is given by the difference between k_1 and k_{-1}. Second, reaction cannot go to completion in either direction but an equilibrium situation must be reached in which the rates of forward and back reaction are equal. If the idea of microscopic reversibility is applicable also to solid state reactions, and it seems entirely reasonable that it should be then an additional constraint must be present. Thus the first of the above consequences could still apply and the net rate be given by the difference between the rates of forward and back reaction. However, the second consequence could not apply. Under conditions of thermodynamic equilibrium, solid state reactions and transitions must, in general, proceed to completion in one direction or another. If not, this would incur a violation of the phase rule. To show this, consider the example of the $\beta \rightleftharpoons \gamma$ transition in Li_2ZnSiO_4, mentioned above. Since Li_2ZnSiO_4 is a congruently melting, thermodynamically stable phase, it may be treated as a one-component system

($C = 1$) and therefore in the absence of the vapour phase and at ambient pressure, the system is subject to the condensed phase rule, $P + F = C + 1 = 2$. Hence the coexistence of two phases ($P = 2$) can occur *only* at a fixed point, $T_c(F = 0)$. At all other temperatures, one or other of the polymorphs β, γ is stable. Such considerations have therefore led to the suggestion that in solid state reactions and transitions microscopic reversibility may be involved, but subject to the constraint that the phase rule is obeyed and that, in general, reactions proceed to completion.

12.8 Crystal chemistry and phase transitions

12.8.1 Structural changes with increasing temperature and pressure

From an understanding of the thermodynamic changes that occur at phase transitions (Fig. 12.4), it is possible to understand, and to a certain degree predict, the changes in crystal structure that occur at phase transitions. Thermodynamic considerations tell us that: *an increase in volume and entropy accompany first-order transitions from low temperature to high temperature polymorphs.* There are several structural consequences of this:

(a) High temperature phases have more open structures and often the atoms or ions have a lower coordination number.
(b) High temperature structures are more disordered.
(c) High temperature structures often have higher symmetry.

A similar set of guidelines may be given for pressure-induced transitons. From Le Chatelier's principle, *a decrease in volume accompanies first-order transitions from low pressure to high pressure polymorphs.* When the pressure term is not negligible, a PV term must be included in the Gibbs free energy and at the transition we have:

$$\Delta G = \Delta U + P\Delta V - T\Delta S = 0$$

Therefore,

$$\Delta U + P\Delta V = T\Delta S$$

In order to balance a decrease in volume, the internal energy, U, must increase and/or the entropy, S, must decrease. The structural consequences of this are, therefore:

(a) High pressure phases have more dense structures and often the atoms or ions have increased coordination number.
(b) High pressure phases have more ordered structures.

On comparing the structural effects of P and T at a transition, we can say that, to a first approximation, the structural consequences of increasing temperature are similar to those of decreasing pressure. Quantitative predictions are difficult

to make, especially with more complex structures, but these guidelines are, nevertheless, very useful.

As examples, for simple AB compounds, the following types of change may be expected:

CsCl structure, CN = 8 $\underset{\text{incr. } P\text{(c)}}{\overset{\text{incr. } T\text{(a)}}{\rightleftarrows}}$ NaCl structure, CN = 6 $\underset{\text{incr. } P\text{(d)}}{\overset{\text{incr. } T\text{(b)}}{\rightleftarrows}}$ ZnS structure, CN = 4

Examples, taken from Rao and Rao (1978), are:

(a) CsCl (479 °C), NH_4Br (179 °C)
(b) MnS
(c) KCl (19.6 kbar), RbCl (5.7 kbar)
(d) ZnO (88.6 kbars), CdS (17.4 kbar).

For AB_2 compounds the following sequences are possible:

Distorted rutile structure (cation CN ~ 5, monoclinic)

$\downarrow$ incr. T(a)

rutile structure (cation CN = 6, tetragonal) $\underset{\text{incr. } T\text{(d)}}{\overset{\text{incr. P (c)}}{\rightleftarrows}}$ quartz structure (cation CN = 4)

$\downarrow$ incr. T(b)

fluorite structure (cation CN = 8)

Examples are:

(a) VO_2, NbO_2
(b) SiO_2 (120 kbar)
(c) GeO_2 (1049 °C)

These latter examples are not quite as straight forward as for the AB compounds because coordination numbers may either increase, or decrease (c) with temperature, but the other guidelines still apply.

12.8.2 Martensitic transformations

Martensitic transformations are a special kind of transformation which occur in a variety of metallic and non-metallic systems. Martensite was the name originally given to the hard material obtained during the quenching of steels; it forms by transformation of austenite, the face centred cubic solid solutions of carbon in γ-Fe (Fig. 11.20). Austenite is unstable below 723 °C and should, under equilibrium conditions, decompose to a mixture of α-Fe and cementite, Fe_3C. On quenching austenite, this eutectoid decomposition reaction is suppressed and, instead, the undercooled, cubic austenite transforms to a metastable tetragonal phase martensite.

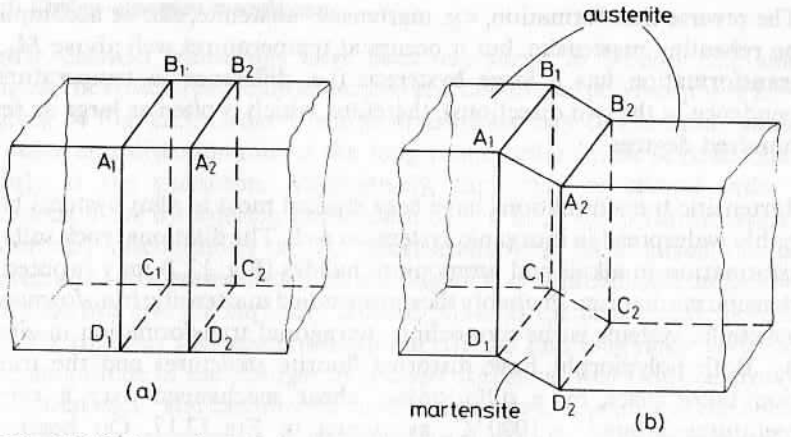

Fig. 12.16 Formation of a martensite plate within a parent austenite crystal

The austenite–martensite transformation is depicted in Fig. 12.16. A crystal of austenite, γ-Fe, is shown in Fig. 12.16 (a). Part of the crystal, between the cross-sections $A_1B_1C_1D_1$ and $A_2B_2C_2D_2$, changes shape by a shearing process on transforming to the martensite structure (Fig. 12.16b). Martensitic transformations have the following characteristics, some or all of which are usually observed:

(a) Transformation occurs by a shearing mechanism to give plates of product crystal within the parent crystal. At the parent–product interfaces, $A_1B_1C_1D_1$ and $A_2B_2C_2D_2$, which are known as *habit planes*, the structures match well and there is a definite orientation relationship between the crystal structures of the two phases. The sizes of the martensite plates are often large enough to be seen with an optical microscope.
(b) The parent and product phases have the same composition and their crystal structures are closely related. Small atomic displacements, often less than one bond length, are necessary to accomplish the transformation and hence the transformations do not involve diffusion.
(c) Because there is no activation energy for diffusion involved, the transformation rates are very high. The parent–product interfaces are said to be *glissile* since they can move without thermal activation. Transformation rates are often independent of temperature, in which case the transformation is said to be *athermal*, but may be affected by applied stresses and strains.
(d) Fig. 12.16(b) shows a partly formed martensite crystal. Unlike other phase transitions, martensitic transformations do not proceed to completion at a constant temperature but take place over a wide range of temperatures. On cooling, martensitic transformations begin to occur at a temperature, M_s, and the extent of transformation usually depends on the degree of cooling below M_s. At a certain lower temperature, M_f, the transition is complete. At temperatures between M_s and M_f, the degree of transformation can be increased by applying shearing stresses to the crystal.

(e) The reverse transformation, e.g. martensite–austenite, can be accomplished on reheating martensite, but it occurs at temperatures well above M_S. The transformation has a large hysteresis (i.e. difference in temperature dependence in the two directions), therefore, which is often as large as several hundred degrees.

Martensitic transformations have been studied most in alloy systems but are probably widespread in inorganic systems as well. The dilational rock salt–CsCl transformation in alkali and ammonium halides (Fig. 12.2) may proceed by a martensitic mechanism. Probably the most studied martensitic transformation in non-metallic systems is the monoclinic–tetragonal transformation in zirconia, ZrO_2. Both polymorphs have distorted fluorite structures and the transformation takes place by a diffusionless, shear mechanism over a range of temperatures around $\sim 1000\,^{\circ}C$, as shown in Fig. 12.17. On heating the monoclinic phase which is stable at low temperatures, transformation to the tetragonal phase begins above $\sim 1000\,^{\circ}C$ but is not complete until $\gtrsim 1120\,^{\circ}C$. The transformation exhibits a hysteresis of about $200\,^{\circ}C$ and the reverse transformation on cooling begins at only $\lesssim 930\,^{\circ}C$. Since the high temperature tetragonal phase cannot normally be quenched to room temperature, the transformation characteristics, as shown in Fig. 12.17, have to be determined directly at high temperatures. Various methods may be used, including high temperature X-ray diffraction, dilatometry, resistivity measurements and DTA. The transformation is classified as athermal because it takes place over a range of temperatures and the percentage transformation within that range does not change with time as long as the temperature remains constant. On changing the temperature, the new 'equilibrium' state is reached extremely rapidly; growth of the product phase by movement of the coherent interface between monoclinic and tetragonal domains occurs at velocities approaching the speed of sound.

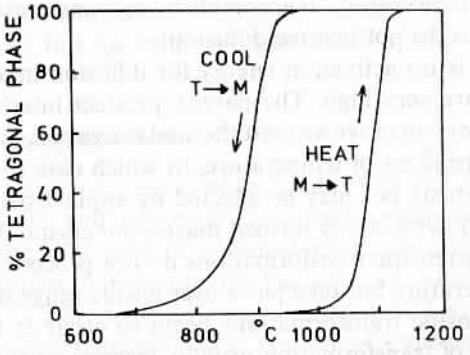

Fig. 12.17 Monoclinic (M)–tetragonal (T) martensitic transformation in zirconia determined by high temperature powder X-ray diffraction (After Wolten, 1963)

12.8.3 Order–disorder transitions

Order–disorder transitions have been mentioned in Section 12.2 and, as examples, the structures of cation ordered and disordered polymorphs of $LiFeO_2$ are given in Fig. 12.3. Order–disorder transitions may be thermodynamically first order and discontinuous if the long range order in the crystals changes abruptly at the transition. Alternatively, they may be second order and continuous if the disordering takes place over a large temperature range and without any discontinuity at T_c. Most transitions have mixed character, however, and show premonitory disordering as T_c is approached from below (or, equally, do not give a completely ordered phase as the temperature is reduced below T_c), together with discontinuities in ΔH, ΔS and long range order at T_c.

The magnitude of the changes in entropy correlates well with the structural changes that occur and can often be used to determine the nature of the disorder. The change in entropy at a transition is made up of contributions from configurational, rotational, vibrational and electronic effects but usually configurational entropy is the major factor. Its value may be calculated if the structures of ordered and disordered polymorphs are known, e.g. AgI transforms from wurtzite-like (β) to a body centred cubic (α) structure at $145\,^{\circ}C$ and the entropy increases by $\sim 14.5\,J\,mol^{-1}\,K^{-1}$ (Section 13.2.2.1) at the transition. In β-AgI, the hexagonal unit cell contains two Ag^+ ions located on specific tetrahedral sites but in α-AgI, the two Ag^+ ions are distributed at random over twelve tetrahedral positons. The change in entropy at the transition is given by

$$\Delta S = k \ln\left(\frac{n_2}{n_1}\right)^N = R \ln\left(\frac{n_2}{n_1}\right) \qquad (12.23)$$

where k is Boltzman's constant, R the gas constant, N Avogadro's number and n_2, n_1 the number of configurations in the two polymorphs. In α-AgI, an Ag^+ ion can be placed in any one of twelve positions but in β AgI, only two positions are available. Therefore, $n_2 = 12, n_1 = 2$ and $\Delta S = R \ln 6 = 14.7\,J\,mol^{-1}K^{-1}$, in good agreement with the experimental value.

Entropy measurements have been particularly useful in evaluating the type of disorder in orientational order–disorder transitions. For example, crystalline KCN contains the cigar-shaped CN^- ion. KCN undergoes two transitions with measured entropies approximately as shown:

$$\text{III} \xrightarrow[\Delta S = R\ln 2]{83\,K} \text{II} \xrightarrow[\Delta S = R\ln 4]{168\,K} \underset{\text{cubic}}{\text{I}}$$

For III → II, $n_2/n_1 = 2$ and the CN^- ion can adopt two possible orientations in polymorph II. For II → I, $n_2/n_1 = 4$ and, therefore, CN^- can adopt any of eight orientations. Polymorph I has a CsCl derivative structure and it appears that the CN^- at the cube body centre can orient along any of eight ⟨111⟩ body diagonal directions.

NH_4Cl undergoes a phase transition that involves reorientation of the

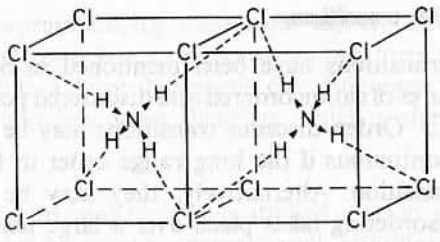

Fig. 12.18 Two possible orientations for NH_4^+ ions in phase II of NH_4Cl (After Rao and Rao, 1978)

NH_4^+ ions; it was thought originally that free rotation of the NH_4^+ ion occurred in the high temperature phase but entropy measurements indicate that this is unlikely. The transition is

$$\underset{\text{CsCl derivative}}{\text{III}} \xrightarrow[\Delta S = R\ln 2]{243\text{ K}} \underset{\text{CsCl derivative}}{\text{II}}$$

In phase III, NH_4^+ ions at the body centre position of the CsCl structure adopt the same orientation in all unit cells, e.g. one of the two orientations shown in Fig. 12.18. In phase II, two different orientations of NH_4^+ occur, as in Fig. 12.18, and these are arranged at random throughout the structure. The measured entropy change corresponds to $\Delta S = R \ln 2$, indicating two orientations of NH_4^+ in phase II. If free rotation of NH_4^+ occurred in phase II, a much larger entropy change would be required. Further polymorphic changes in NH_4Cl occur at higher temperatures.

Questions

12.1 How would you classify the following phase transitions: (a) quartz → cristobalite, SiO_2; (b) rutile → quartz, GeO_2; (c) tetragonal → monoclinic ZrO_2; (d) diamond → graphite; (e) ferroelectric → paraelectric $BaTiO_3$ (Chapter 15).

12.2 Using the data given in Table 12.2, calculate the entropies of the transitions: (a) low → high quartz; (b) $\beta \rightarrow \alpha$ AgI; (c) monoclinic → cubic Li_2SO_4. Comment on the relative magnitudes of your results.

12.3 What kind of structural changes, if any, might you expect the following to undergo as a consequence of (a) increasing temperature, (b) increasing pressure: (i) SiO_2; (ii) ZnO; (iii) SnO_2 (rutile structure); (iv) NH_4I?

12.4 The heat of fusion of tin metal is 61 J gm^{-1}. What is the change in free energy when 1 mole of tin melts at the equilibrium melting temperature? What is the corresponding entropy change?

References

M. J. Buerger (1961, 1972). Polymorphism and phase transformations, *Fortschr. Miner.*, **39** (1), 9–24; *Soviet Physics—Crystallography*, **16** (6) 959–968.

S. Flandrois (1974). Kinetics of phase changes in the solid state, *J. Chim. Physique*, **71** (6), 979–991.

H. Henisch, R. Roy and L. E. Cross (Eds) (1973). *Phase Transitions*, Pergamon Press, New York.

H. Lipson (1950). Order–disorder changes in alloys, in *Progress in Metal Physics* (Ed. B. Chalmers), Vol. II, Butterworths.

H. Moser (1936). *Phys. Z.*, **37**, 737.

C. N. R. Rao and K. J. Rao (1978). *Phase Transitions in Solids*, McGraw-Hill.

K. J. Rao and C. N. R. Rao (1966). *J. Materials Sci.*, **1**, 238.

R. Smoluchowski (Ed.) (1951). *Phase Transformations in Solids*, Wiley, New York.

E. C. Subbarao, H. S. Maiti and K. K. Srivastava (1974). Martensitic transformation in zirconia, *Phys. Stat. Sol.*, **A21**, 9.

A. R. Ubbelohde (1957). Thermal transformations in solids, *Quart. Rev. (London)*, **11**, 246.

M. E. Villafuerte-Castrejon and A. R. West (1981). *J. Chem. Soc. Faraday* 1, **77**, 2297.

A. R. West (1975). *Z. Krist.*, **141**, 422.

G. M. Wolten (1963). *J. Amer. Ceram. Soc.*, **46**, 418.